www.rsc.org/materials |
Journal of Materials Chemistry

Enzymatic sensing with organic electrochemical transistors

Daniel A. Bernards, Daniel J. Macaya, Maria Nikolou, John A. DeFranco, Seiichi Takamatsu and George G. Malliaras*

Received 28th August 2007, Accepted 3rd October 2007
First published as an Advance Article on the web 12th October 2007
DOI: 10.1039/b713122d

Since their development in the 1980's organic electrochemical transistors (OECTs) have attracted a great deal of interest for biosensor applications. Coupled with the current proliferation of organic semiconductor technologies, these devices have the potential to revolutionize healthcare by making point-of-care and home-based medical diagnostics widely available. Unfortunately, their mechanism of operation is poorly understood, and this hinders further development of this important technology. In this paper glucose sensors based on OECTs and the redox enzyme glucose oxidase are investigated. Through appropriate scaling of the transfer characteristics at various glucose concentrations, a universal curve describing device operation is shown to exist. This result elucidates the underlying device physics and establishes a connection between sensor response and analyte concentration. This improved understanding paves the way for rational optimization of enzymatic sensors based on organic electrochemical transistors.

1. Introduction

The field of organic electronics is in the midst of tremendous development, with organic semiconductors being considered for applications in electronic and optoelectronic devices, including light emitting diodes, photovoltaic cells, and thin-film transistors.[1] Key advantages of these materials include tunability of their electronic properties *via* chemical synthesis and compatibility with roll-to-roll fabrication, which can yield ultra-low cost manufacturing. An emerging focus in the field involves the use of organic-based devices as transducers in chemical and biological sensors.[2–6] In particular, organic thin-film transistors (OTFTs) are attracting a great deal of interest for sensor applications due to their simple electrical readout, inherent signal amplification, straightforward miniaturization, and facile incorporation into arrays and circuits. To date, OTFTs have been used to sense mechanical deformation and pressure, humidity and organic vapors, pH and ion concentrations, and a variety of biologically relevant analytes.[2–7]

Within the family of organic semiconductor-based sensors, organic electrochemical transistors (OECTs—also known as conducting polymer transistors) have attracted particular interest.[2,4] These devices were first developed in the 1980s by the group of Wrighton[8–10] and rapidly found application in sensors.[9–11] Unlike the majority of OTFTs, which are field-effect devices that rely on electrostatic gating, OECT operation relies on electrochemical doping/de-doping of an organic semiconductor film in contact with an electrolyte. This results in lower operating voltages, which make OECTs particularly suitable for biological and chemical detection in aqueous environments. The intimate contact between organic semiconductor and electrolyte in these devices makes them an excellent intermediary between the fields of biology and electronics: these devices have been used as ion-to-electron converters,[12] have been integrated with cell membranes,[13] and, more recently, have been used as ion pumps promoting cell growth.[14] Their simple structure allows for fabrication using roll-to-roll techniques[15] and lends itself to easy integration with microfluidic channels for lab-on-a-chip applications.[16]

Cornell University, Ithaca, NY, USA. E-mail: ggm1@cornell.edu; Fax: 607 255 2365; Tel: 607 2551956

2. Materials and methods

The commercially available PEDOT:PSS Baytron P was used as the active material for the fabrication of the OECTs. It was deposited on glass slides and patterned using the parylene technique described by DeFranco *et al.*[17] Chemical vapor deposition was used to deposit 1.5 μm films of parylene on glass. Conventional lithography followed by an oxygen plasma etch was used to pattern the parylene film. Excess resist was removed with acetone. Prior to spin coating, the glass slides were treated with an oxygen plasma to improve film adhesion. A mixture of Baytron P and ethylene glycol (4 : 1 by volume) was spin cast at 1500 rpm onto the patterned support. Ethylene glycol was used to improve the conductivity of the PEDOT:PSS films. A small amount ($\sim$5 μL mL^{-1}) of dodecylbenzenesulfonic acid (DBSA) was added as a surfactant to improve film formation. The parylene film was then peeled from the glass support, leaving 1 mm wide PEDOT:PSS stripes. Devices were first baked on a hotplate for 20 s at 140 °C and then baked under vacuum at 140 °C for 1 h. PEDOT:PSS films were then soaked in de-ionized water to remove any surface contamination. Sylgard 184, poly(dimethylsiloxane) (PDMS), was used to confine the electrolyte to a 4 mm × 10 mm area over the PEDOT:PSS stripes. Sylgard 184 was mixed at a 20 : 1 base to cross-linker ratio and cured at 60 °C for 1 h prior to being used. The active PEDOT:PSS device area was 1 mm × 10 mm. A platinum wire was used as the gate electrode. All measurements were made with Keithley 2400 SourceMeters. Devices were tested using a fixed $V_d = -0.2$ V with V_g = 0, 0.1, 0.2, and 0.4 V. A 0.15 mM phosphate

buffered saline (PBS) was used as the electrolyte for all experiments, which had a pH of 6.8 as measured by pH meter. Different concentrations of glucose in PBS were achieved by mixing a 50 μL solution of PBS and glucose with 50 μL solution of PBS and glucose oxidase (500 units mL^{-1}).

3. Results and discussion

Fig. 1a shows the typical configuration of an OECT. The transistor consists of an organic semiconductor film and an electrolyte with a gate electrode immersed in it. A common organic semiconductor material used in contemporary OECTs is poly(3,4-ethylenedioxythiophene) doped with poly(styrenesulfonate) (PEDOT:PSS). This is a degenerately doped p-type organic semiconductor (also referred to as a conducting polymer), in which hole transport takes place in the PEDOT phase while the PSS phase supports the sulfonate acceptors. The overlap of the electrolyte with the organic semiconductor defines the transistor channel, where the electrolyte is contained by a poly(dimethylsiloxane) (PDMS) well. Source and drain electrodes make electrical contact to the organic semiconductor film and the gate electrode is immersed in the electrolyte. By convention, the source electrode is grounded, a small bias is applied on the drain electrode (V_d), and the source–drain current (I_{sd}) that flows through the channel is measured. The latter is modulated by a voltage applied to the gate electrode (V_g). For the case of p-type materials such as PEDOT:PSS, application of a positive V_g causes positive ions from the electrolyte to enter the organic film and de-dope it, decreasing the source–drain current.[18] Therefore, PEDOT:PSS OECTs operate in depletion mode (*i.e.* as gate voltage increases, source–drain current decreases). De-doping in these devices is reversible, and the source–drain current recovers when V_g is returned to zero.

Soon after the demonstration of the first OECT, these devices found use as transducers in biological sensors—in particular, coupled with redox enzymes for the detection of metabolites.[19–24] Metabolite levels are an important diagnostic marker in healthcare since they often correspond to physiological irregularities that warrant treatment or further investigation. Enzymes are excellent recognition elements for metabolites since they specifically react with these and do not suffer from significant interference. The use of redox enzymes, in particular, can provide versatility in the output signal and enhance the range of sensing possibilities. For sensor applications, enzymes can be blended with or chemically linked to the organic semiconductor or gate electrode,[19–22] or introduced free-floating into the electrolyte.[23,24] When the appropriate analyte is present in the electrolyte, its interaction with the enzyme modulates the source–drain current. A calibration curve that correlates the relative change in I_{sd} to analyte concentration can be generated and subsequently used to deduce unknown analyte concentrations.

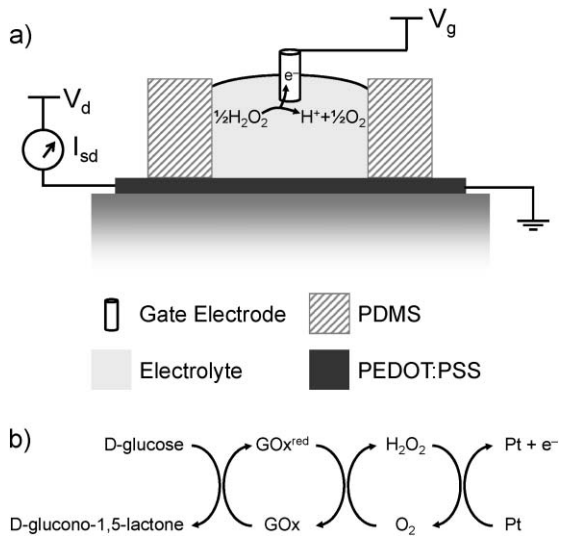

Fig. 1 (a) Schematic of a typical organic electrochemical transistor (not to scale). The reaction of interest is shown at the gate electrode. (b) Reaction cycle involved in the detection of glucose using GOx.

Despite the large interest in the application of OECTs for enzymatic sensing and the potential of these devices to make a major contribution to healthcare, the operational mechanism for these devices is not understood in real detail. For example, it is not clear how sensor metrics, such as sensitivity, relate to materials' properties and device parameters. This hinders further development and deployment of these devices. In this paper we describe experiments that elucidate the physics underlying OECT operation and connect device response to analyte concentration in OECT-based enzymatic sensors.

The fruit fly of enzymatic sensing involves the detection of glucose using glucose oxidase (GOx). The reaction cycle involved is show in Fig. 1b. GOx catalyzes the conversion of D-glucose to D-glucono-1,5-lactone and is reduced in the process. Reactivation of GOx from its reduced state produces hydrogen peroxide. Since the concentration of peroxide is directly related to the concentration of glucose, peroxide is often used to detect and measure the concentration of glucose. A Pt electrode immersed in the electrolyte can catalyze the decomposition of peroxide:

$$H_2O_2 \rightarrow 2H^+ + O_2 + 2e^- \quad (1)$$

Glucose can be sensed with a PEDOT:PSS OECT using a Pt gate electrode and an electrolyte (in this case phosphate buffered saline) with free-floating GOx. Introduction of glucose into the electrolyte results in the reactions described above and consequently affects the source–drain current. This is shown in Fig. 2a, where the transistor transfer characteristics are plotted for different glucose concentrations. All curves show a monotonic decrease of the source–drain current with increasing gate voltage due to de-doping of the organic semiconductor. With increasing glucose concentration, however, the magnitude of the modulation increases. The presence of glucose clearly affects electrical characteristics, but the mechanism responsible for these changes is not clear.

Essential to understanding the mechanism of operation is the observation that the data in Fig. 2a can be scaled to yield a universal curve. This is shown in Fig. 2b, where the gate voltage was scaled according to:

$$V_g^{eff} = V_g + V_{offset} \quad (2)$$

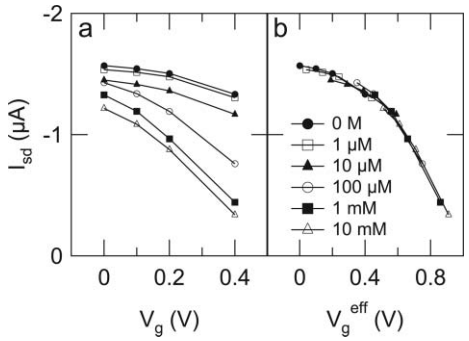

Fig. 2 (a) Source–drain current plotted as a function of applied gate voltage for a fixed drain voltage (V_d = −0.2 V) and various glucose concentrations. (b) Source–drain current plotted as a function of effective gate voltage, where the applied gate voltage is shifted by an offset voltage (V_{offset}) that depends on concentration. V_{offset} is chosen such that the measured current lies along a universal curve, where the extent of the shift is determined by glucose concentration.

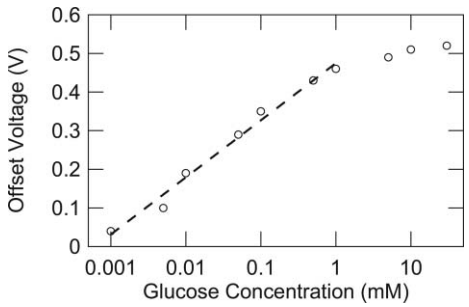

Fig. 3 Dependence of the offset voltage on glucose concentration. The solid line is a fit to the data up to a glucose concentration of 1 mM.

where V_g^{eff} is the effective gate voltage and V_{offset} is an offset voltage that is dependent on glucose concentration. The curve in Fig. 2b agrees with the typical transfer characteristics of a depletion mode transistor,[25] showing the expected decrease of source–drain current on drain voltage. The effect of glucose concentration on transistor response is illustrated in Fig. 3, which displays V_{offset} as a function of glucose concentration. A logarithmic dependence is observed for glucose concentrations up to 1 mM, above which it tapers off.† This shows that the presence of glucose has a systematic effect on the gating of the transistor. A logarithmic behavior is reminiscent of the Nernst equation, which describes the dependence of the chemical potential on the concentration of redox-active species:[26]

$$E_{Nernst} = E^{0'} + \frac{kT}{ne}\ln\left(\frac{[Ox]}{[Red]}\right) \quad (3)$$

where [Ox] and [Red] are the concentrations of oxidized and reduced species, respectively, $E^{0'}$ is the formal potential, k is Boltzmann's constant, T is the temperature, e is the fundamental charge, and n is the number of electrons transferred during the reaction.

† In this case, saturation of V_{offset} is due to insufficient sampling time—steady state operation is increasingly difficult to obtain as depletion increases.

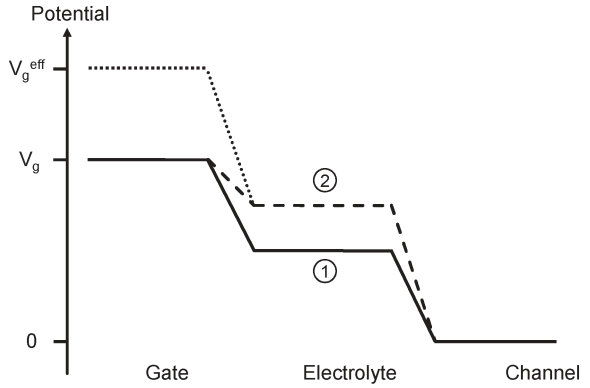

Fig. 4 Potential diagram of the OECT. In the absence of glucose (solid line), the electrolyte potential (1) is determined by the relative capacitances at the gate and channel interfaces. In the presence of glucose (dashed line), the electrolyte potential (2) is increased according to the Nernst equation. The effective gate voltage (dotted line) is the gate voltage required to produce the same electrolyte potential (2) in the absence of Faradaic effects. The lines connecting gate, electrolyte, and channel potentials are meant as guides to the eye.

In order to understand the physical meaning of the offset voltage one needs to consider a comparison between OECTs and sensors based on conventional electrochemical detection. In conventional electrochemistry, the effects of the Nernst equation are manifested in changes of the potential at a working electrode (where the reaction occurs) relative to a reference electrode potential. In contrast, the potential of the gate electrode in an OECT is fixed. Consequently, the potential shift described by the Nernst equation is manifested by a shift of the electrolyte potential relative to that of the gate. This alternate but physically equivalent reference frame is shown in Fig. 4. For simplicity V_d was assumed to be small compared to V_g so that the entire channel is effectively grounded. In the absence of glucose, peroxide is not generated and the reaction shown in eqn (1) does not take place.

Moreover, for gate voltages that are small enough to prevent electrolysis of water, there is no charge transfer between the electrolyte and the Pt electrode (non-Faradaic regime). The electrolyte potential in this case is determined by the capacitances associated with double layer formation at the gate and the channel (solid line in Fig. 4) and is equal to:

$$V_{sol}^{(1)} = \frac{V_g}{1+\gamma} \quad (4)$$

where γ is the capacitance ratio (defined as $\gamma = C_c/C_g$, where C_c and C_g are the channel and gate capacitances, respectively). When glucose is added to the electrolyte, electrons flow onto the Pt electrode according to the reaction shown in eqn (1), and the potential drop at the Pt–electrolyte interface decreases as a result. This Faradaic contribution is described by the Nernst equation; given that the potential of the gate electrode is held constant, the potential of the electrolyte is:

$$V_{sol}^{(2)} = \frac{V_g}{1+\gamma} + \frac{kT}{2e}\ln[H_2O_2] + \text{constant} \quad (5)$$

where the constant contains the details of proton and oxygen concentrations and the formal potential. This new value of the

electrolyte potential is illustrated in Fig. 4 with a dashed line. In deriving eqn (5) it was assumed that the electrolyte is buffered (*i.e.* proton concentration is constant) and that the device is open to the atmosphere (*i.e.* the oxygen in the electrolyte is at its equilibrium concentration). In both eqn (4) and (5), it was assumed that V_d is small compared to V_g, hence the entire channel can be considered grounded.

The current that flows in the channel of an OECT for a particular drain voltage depends only on the potential of the electrolyte, and the details at the gate electrode can be neglected. This was recently demonstrated in carbon nanotube electrochemical transistors,[27] where a reference electrode was used to monitor the potential of the electrolyte. From eqn (5) it is clear that the addition of glucose increases the electrolyte potential and correspondingly decreases the source–drain current. It is convenient to define an effective gate voltage:

$$V_g^{eff} = V_g + (1+\gamma)\frac{kT}{2e}\ln[H_2O_2] + \text{constant}^* \quad (6)$$

where the new constant is that of eqn (5) multiplied by $(1 + \gamma)$. V_g^{eff} is the equivalent voltage that needs to be applied in the absence of Faradaic effects at the gate electrode in order to result in the same source–drain current. V_g^{eff} is illustrated in Fig. 4 with a dotted line.

The above analysis also clarifies the physical meaning of the offset voltage involved in the transformation shown in Fig. 2. V_{offset} is represented by the last two terms in eqn (6) and describes the Faradaic contribution to the effective gate voltage. It originates from the shift in the chemical potential described by the Nernst equation and is scaled by the capacitance ratio. The line in Fig. 3 is a fit to V_{offset} with γ = 4. Given that the capacitance of polymer electrodes is greater than that of metals per unit area[28] and that the area of the gate electrode was smaller than that of the channel, a value for γ that is larger than one is reasonable. It should be noted that the capacitance associated with metals and polymers is mechanistically distinct: while metals such as Pt are impermeable to ionic charge, ions can penetrate polymers[12] (although this is not always the case[29]), which gives rise to a unique origin for the capacitance in each.[30] The potential drop between the electrolyte and the channel in Fig. 4 implies ion accumulation on the surface of the PEDOT:PSS. An effective capacitance can still be used for the case where ions completely penetrate the PEDOT:PSS.

According to the above, OECTs can be viewed as remote voltage sensors. Charge transfer reactions that alter the potential near the gate electrode can be detected by measuring the source–drain current in the organic semiconductor film. Despite its indirect nature, this mode of detection lends itself to uncomplicated, high-sensitivity transduction. Changes in the source–drain current can be easily measured with high accuracy and only require simple equipment.

Bernards and Malliaras have shown that the source–drain current in OECTs for the case of uniform de-doping is given by:[18]

$$I_{sd} = \frac{G}{V_p}\left(V_p - V_g^{eff} + \tfrac{1}{2}V_d\right)V_d \quad (7)$$

and, in the saturation regime, by:[18]

$$I_{sd} = -\frac{G}{2V_p}\left(V_g^{eff} - V_p\right)^2 \quad (8)$$

where G is the conductance of the organic semiconductor film and V_p is the pinch-off voltage (determined by materials and device parameters). Incorporation of the effective gate voltage in the equations above yields a quantitative relationship between the source–drain current and the glucose concentration. The relevant constants can be easily extracted from materials properties (such as the conductivity of PEDOT:PSS) and device parameters.

Fig. 5 demonstrates the validity of the analysis presented in this paper. The normalized response (NR) of the source–drain current is plotted as a function of glucose concentration and gate voltage. Normalization was done relative to the zero concentration limit as:

$$NR = \left|\frac{I_{sd}^{conc} - I_{sd}^{conc=0}}{I_{sd}^{conc=0}}\right| \quad (9)$$

where I_{sd} is considered at zero concentration and at the concentration of interest. This normalization provides a maximum range of response from zero (no analyte) to one (upper concentration limit) and facilitates comparison between different devices. Fig. 5 shows experimental data (filled circles) from PEDOT:PSS OECTs fit to eqn (6–8) with γ = 4, V_p = 0.8 V, and with a correction for the resistivity of the source and drain electrodes. It should be noted that a sensor response is observed experimentally at zero gate voltage. However, the model described above cannot be used in this regime as it assumes V_d to be small compared to V_g.

The excellent agreement between theory and measurement in Fig. 5 illustrates that the analysis described above can quantitatively describe the operation of OECT-based enzymatic sensors. This paves the way for the rational design of better devices and helps explain some of the unique characteristics of OECTs. One example is the increase of sensitivity (slope of NR *versus* glucose concentration) with gate voltage

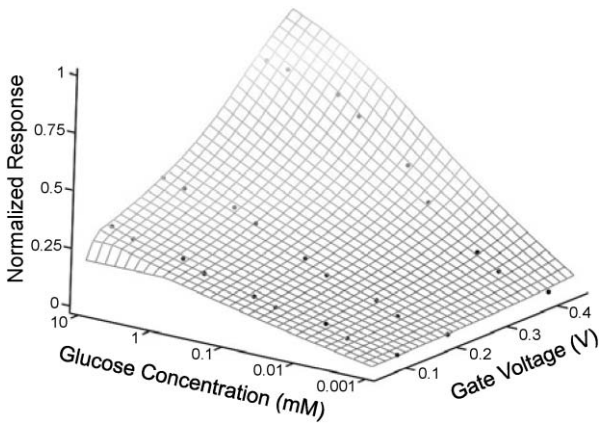

Fig. 5 Normalized response of the source–drain current as a function of applied gate voltage and glucose concentration. Filled circles are experimental data and the grid is a fit.

(Fig. 5). It can be shown that this arises from a term in NR that is proportional to:

$$\frac{\log(H_2O_2)}{V_p - V_g + 1/2 V_d}$$

and therefore increases with gate voltage. It is also possible to tune the NR by varying γ through device geometry or material selection.

4. Conclusions

The behavior of OECT-based enzymatic sensors was investigated. PEDOT:PSS was used as the conducting polymer, and the redox enzyme glucose oxidase was introduced to the electrolyte of the OECT in order to detect glucose. Appropriate scaling of the transistor transfer characteristics at various glucose concentrations yielded a universal curve of the source–drain current *versus* effective gate voltage. This observation helped elucidate the physics of OECT-based enzymatic sensors. An effective gate voltage was used to account for Faradaic contributions to the potential at the gate electrode. A connection between source–drain current and analyte concentration was developed and resulted in an excellent fit to experimental data. This improved understanding paves the way for rational optimization of OECT-based enzymatic sensors.

Acknowledgements

We thank Burak Ulgut and Héctor Abruña for suggestions and comments regarding this work. D.A.B. thanks the United States Department of Defense for a fellowship. This work was supported by the Center for Nanoscale Systems, and was partly performed in the Cornell NanoScale Science and Technology Facility, which is funded by the National Science Foundation and the New York State Office of Science, Technology & Academic Research.

References

1 G. Malliaras and R. Friend, *Phys. Today*, 2005, **58**, 53.
2 L. Wang, D. Fine, D. Sharma, L. Torsi and A. Dodabalapur, *Anal. Bioanal. Chem.*, 2005, **384**, 310.
3 J. Locklin and Z. Bao, *Anal. Bioanal. Chem.*, 2005, **384**, 336.
4 J. T. Mabeck and G. G. Malliaras, *Anal. Bioanal. Chem.*, 2005, **384**, 343.
5 C. Bartic and G. Borghs, *Anal. Bioanal. Chem.*, 2005, **384**, 354.
6 M. Bouvet, *Anal. Bioanal. Chem.*, 2005, **384**, 366.
7 T. Someya, T. Sekitani, S. Iba, Y. Kato, H. Kawaguchi and T. Sakurai, *Proc. Natl. Acad. Sci. U. S. A.*, 2004, **100**, 9966.
8 H. S. White, G. P. Kittlesen and M. S. Wrighton, *J. Am. Chem. Soc.*, 1984, **106**, 5375.
9 E. W. Paul, A. J. Ricco and M. S. Wrighton, *J. Phys. Chem.*, 1985, **89**, 1441.
10 J. W. Thackeray, H. S. White and M. S. Wrighton, *J. Phys. Chem.*, 1985, **89**, 5133.
11 J. W. Thackeray and M. S. Wrighton, *J. Phys. Chem.*, 1986, **90**, 6674.
12 D. Nilsson, M. Chen, T. Kugler, T. Remonen, M. Armgarth and M. Berggren, *Adv. Mater.*, 2002, **14**, 51.
13 D. A. Bernards, G. G. Malliaras, G. E. S. Toombes and S. M. Gruner, *Appl. Phys. Lett.*, 2006, **89**, 053505.
14 J. Isaksson, P. Kjäll, D. Nilsson, N. Robinson, M. Berggren and A. Richter-Dahlfors, *Nat. Mater.*, 2007, **6**, 673.
15 M. Berggren, D. Nilsson and N. D. Robinson, *Nat. Mater.*, 2007, **6**, 3.
16 J. T. Mabeck, J. A. DeFranco, D. A. Bernards, G. G. Malliaras, S. Hocde and C. J. Chase, *Appl. Phys. Lett.*, 2005, **87**, 013503.
17 J. A. DeFranco, B. S. Schmidt, M. Lipson and G. G. Malliaras, *Org. Electron.*, 2006, **7**, 22.
18 D. A. Bernards and G. G. Malliaras, *Adv. Funct. Mater.*, DOI: 10.1002/adfm.200601239.
19 T. Matsue, M. Nishizawa, T. Sawaguchi and I. Uchida, *J. Chem. Soc., Chem. Commun.*, 1991(15), 1029.
20 M. Nishizawa, T. Matsue and I. Uchida, *Anal. Chem.*, 1992, **64**, 2642.
21 D. T. Hoa, T. N. S. Kumar, N. S. Punekar, R. S. Srinivas, R. Lal and A. Q. Contractor, *Anal. Chem.*, 1992, **64**, 2645.
22 A. Q. Contractor, T. N. S. Kumar, R. Narayanan, S. Sukeerthi, R. Lal and R. S. Srinivas, *Electrochim. Acta*, 1994, **39**, 1321.
23 Z. T. Zhu, J. T. Mabeck, C. C. Zhu, N. C. Cady, C. A. Batt and G. G. Malliaras, *Chem. Commun.*, 2004(13), 1556.
24 D. J. Macaya, M. Nikolou, S. Takamatsu, J. T. Mabeck, R. M. Owens and G. G. Malliaras, *Sens. Actuators, B*, 2007, **123**, 374.
25 S. M. Sze, *Physics of Semiconductor Devices*, Wiley, New York, 1981.
26 A. J. Bard and L. R. Faulkner, *Electrochemical Methods*, John Wiley and Sons, New York, 1981.
27 L. Larrimore, S. Nad, X. Zhou, H. Abruna and P. L. McEuen, *Nano Lett.*, 2006, **6**, 1329.
28 J. D. Stenger-Smith, C. K. Webber, N. Anderson, A. P. Chafin, K. Zong and J. R. Reynolds, *J. Electrochem. Soc.*, 2002, **149**, A973.
29 M. J. Panzer and C. D. Frisbie, *J. Am. Chem. Soc.*, 2007, **129**, 6599.
30 J. Wang and A. J. Bard, *J. Am. Chem. Soc.*, 2001, **123**, 498.

